Basic and Tailored RF Shimming in a Multi-transmit Whole Body MR System

U. Katscher
Philips Research Europe, Hamburg, Germany

Abstract— Wave propagation effects diminish the quality of MR images at main fields of 3T or above. Parallel RF transmission has the potential of compensating for these effects through RF shimming. RF shimming can be performed in two different ways. The basic way of RF shimming is to adjust the global amplitude and phase of the currents in each transmit element, aiming at a constant B_1 in the region of interest. For 3D volume imaging, 3D RF shimming is facilitated using multiple frequencies for the different transmit elements. On the other hand, "tailored" RF shimming can be performed via multi-dimensional RF pulses designed to achieve a spatially constant excitation pattern. Using an MR system equipped with parallel RF channels, these multi-dimensional RF pulses can be accelerated via Transmit SENSE.

The potential of both, basic and tailored RF shimming, can be enhanced significantly, if only a constant B_1 amplitude is demanded, and an arbitrary spatial distribution of the resulting B_1 phase is allowed. This is the case, if only magnitude images are of interest. However, this approach introduces a non-linear problem, requiring corresponding numerical techniques.

Optimal results for basic RF shimming are obtained with transmit arrays owning preferably homogeneous sensitivity distributions of the individual elements. On the other hand, for tailored shimming, the transmit elements require orthogonal sensitivity distributions, which are easier to achieve with inhomogeneous sensitivity distributions. Thus, the transmit coil array cannot be optimized for both, basic and tailored RF shimming simultaneously, and a suitable compromise has to be found.

This study compares the different RF shimming approaches using a whole-body, 8-channel Tx/Rx system at 3T. It shows, that basic RF shimming is able to remove B_1 inhomogeneities to a high degree, both in phantoms and in vivo. Tailored RF shimming is able to achieve even higher levels of B_1 homogeneity, which, however, might not be necessary for the majority of clinical applications.

1. INTRODUCTION

Wave propagation effects diminish the quality of MR images at main fields of 3T or above. Parallel RF transmission has the potential of compensating for these effects through RF shimming. RF shimming can be performed in two different ways. The basic way of RF shimming is to adjust the global amplitude and phase of the currents in each transmit element, aiming for a constant B_1 amplitude in the region of interest [1, 2]. For 3D volume imaging, 3D RF shimming is facilitated using multiple frequencies for the different transmit elements [3]. On the other hand, "tailored" RF shimming can be performed via multi-dimensional RF pulses [4], accelerated via parallel transmission [5, 6], designed to achieve a spatially constant excitation pattern [7–9]. This study compares the different RF shimming approaches using a whole-body, 8-channel Tx/Rx system at 3T [10, 11].

2. THEORY

The central equation for both, the basic and tailored RF shimming, is given by

$$\sum_{n=1}^{N} T_n(\mathbf{x}) P_n(\mathbf{x}) = C(\mathbf{x}). \tag{1}$$

This equation states, that the superposition of the transmit sensitivity profiles $T_n(\mathbf{x})$ of the N transmit coils, weighted with $P_n(\mathbf{x})$, yields the desired constant B_1 distribution $C(\mathbf{x}) = const.$ For the basic RF shimming, $P_n(\mathbf{x})$ are constant, leading to a global (complex) scaling of the different sensitivity profiles $T_n(\mathbf{x})$. For 3D volume imaging, 3D RF shimming might be performed via a technique called "Multi-Frequency Excitation" ("MULTIFEX", [3]). Here, the elements of a transmit array are driven with different frequencies to excite different slabs in the excitation volume via the

underlying gradient. Amplitudes and phases can be optimized for each slab individually to achieve maximum B_1 homogeneity. For the tailored RF shimming, $P_n(\mathbf{x})$ of Eq. (1) define spatial excitation patterns of the individual transmit elements, which can be converted to (multi-dimensional) RF pulses [4]. The simultaneous use of multiple transmit elements allows the shortening of the different pulses [5, 6]. By discretizing Eq. (1) on a spatial grid, it can be solved via linear algebra for both basic and tailored RF shimming.

In the majority of applications, only a constant amplitude $|C|$ is required, and an arbitrary spatial phase distribution $\varphi(\mathbf{x})$ is acceptable $C(\mathbf{x}) = const\ \exp(i\varphi(\mathbf{x}))$. This is the case, if only magnitude images are of interest. The resulting degree of freedom enhances the power of (basic and tailored) RF shimming considerably, however, Eq. (1) is no longer linear and corresponding non-linear inversion techniques are required.

Optimal results for basic RF shimming are obtained with transmit arrays showing preferably homogeneous sensitivity distributions of the individual elements. On the other hand, for tailored shimming, the transmit elements require orthogonal sensitivity distributions, which are easier to achieve with inhomogeneous sensitivity distributions. Thus, the transmit coil array cannot be optimized for both, basic and tailored RF shimming simultaneously, and a suitable compromise has to be found.

3. METHODS

Experiments has been performed using a 3T MR system (Philips Achieva, Philips Medical System, The Netherlands) equipped with an 8-element Tx/Rx body coil and corresponding parallel RF channels [10, 11]. Since it is expected that basic RF shimming will be the preferred way of shimming, the transmit elements were designed to be slightly more suitable for basic than for tailored RF shimming. However, the differences are small, and might be outperformed by other system parameters.

The transmit sensitivities have been determined via "Actual Flip angle Imaging" [12]. Basic and tailored RF shimming has been performed as described in the previous section.

For the phantom experiments, a water bottle with a diameter of 20 cm has been used. Images without and with basic RF shimming have been acquired using a FFE sequence with $TR = 8.0$ ms, $TE = 2.6$ ms, a spatial resolution of $1.5 \times 1.5 \times 10\,\mathrm{mm}^3$, and a flip angle of $\alpha = 15°$. Tailored RF shimming has been performed with a reduction factor of $R = 2$ via a spiral k-space trajectory with 8 revolutions for a field of excitation of 32^2 pixels. For the acquisition, a 3D-FFE sequence was used with $TR = 40.0$ ms, $TE = 1.4$ ms, and a spatial resolution of $9 \times 9 \times 10\,\mathrm{mm}^3$.

Furthermore, basic RF shimming has been applied in vivo for mammography. For these experiments, a FFE sequence was chosen with $TR = 4.14$ ms, $TE = 2.0$ ms, a spatial resolution of $1.5 \times 1.5 \times 10\,\mathrm{mm}^3$, and a flip angle of $\alpha = 15°$. Written consent was obtained from all participants of this study.

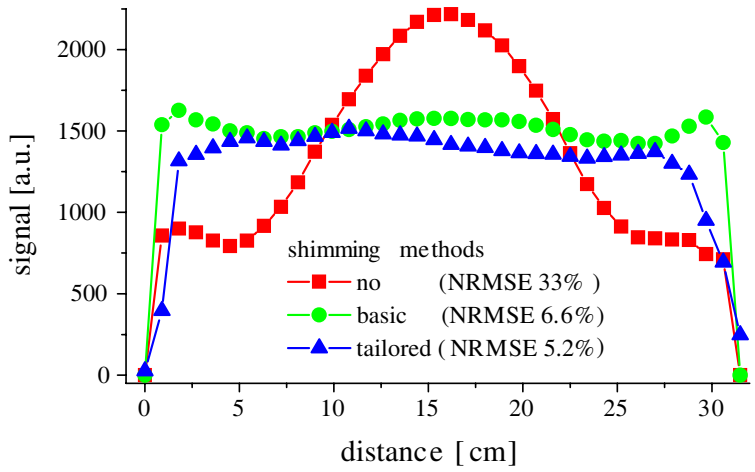

Figure 1: Experimental phantom results. Without shimming, the normalized root-mean square error (NRMSE) is 33% (red line/symbols). The NRMSE reduces to 6.6% for basic (green line/symbols) and 5.2% for tailored shimming (blue line/symbols).

4. RESULTS/DISCUSSION

Experimental phantom results are shown in Fig. 1. Without shimming, the normalized root-mean square error (NRMSE) is 33%. The NRMSE reduces to 6.6% for basic and 5.2% for tailored shimming. Thus, both RF shimming approaches show a high potential to homogenise the overall B_1 transmit field. However, at least for this scenario, the potential of tailored RF shimming seems to be only slightly higher than the potential of basic RF shimming. For Fig. 1, no phase demand was given for basic RF shimming. The solution of the resulting non-linear optimization problem took roughly 35 s on a standard PC. The RF pulses for tailored RF shimming were calculated using a spatially constant phase demand. The solution of the resulting matrix/vector equation took roughly 10 s on a standard PC.

The high potential of basic RF shimming is also found in the framework of the mammography study (Fig. 2). Within the breasts, an NRMSE of 37.4% is found without RF shimming. With basic RF shimming, an NRMSE inside the breasts of 18.7% is found. Thus, using basic RF shimming reduced the left-right signal imbalance of the image significantly.

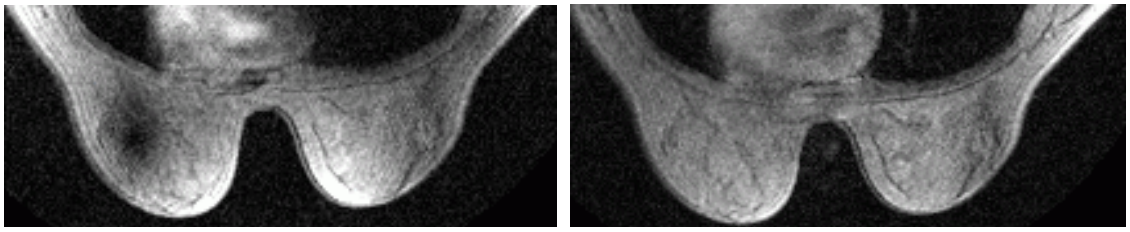

Figure 2: RF shimming for mammography. Left: without RF shimming (NRMSE inside breast = 37.4%). Right: using basic RF shimming (NRMSE inside breasts = 18.7%). The left-right signal imbalance is reduced significantly. It is expected that the small residual inhomogeneities, particularly on the right portion of the torso, will disappear using tailored RF shimming.

5. CONCLUSIONS

Basic RF shimming is able to remove B_1 inhomogeneities to a high degree, both in phantoms in vivo. Tailored RF shimming is able to achieve even higher levels of B_1 homogeneity, which, however, might not be necessary for the majority of clinical applications.

ACKNOWLEDGMENT

The author would like to thank Ingmar Graesslin, Peter Vernickel, Kay Nehrke, and Peter Börnert for their support.

REFERENCES

1. Hoult, D. I. and D. Phil, "Sensitivity and power deposition in a high-field imaging experiment," *J Magn. Reson. Imaging*, Vol. 12, No. 1, 46–67, 2000.
2. Ibrahim, T. S., R. Lee, B. A. Baertlein, A. Kangarlu, and P. L. Robitaille, "Application of finite difference time domain method for the design of birdcage RF head coils using multi-port excitations," *J Magn. Reson. Imaging*, Vol. 18, No. 6, 733–742, 2000.
3. Katscher, U., H. Eggers, I. Graesslin, G. Mens, and P. Börnert, "3D RF shimming using multi-frequency excitation," *16 Proceedings of International Society of Magnetic Resonance in Medicine*, 1263, Toronto, Canada, May 2008.
4. Pauly, J., D. Nishimura, and A. Macovski, "A k-space analysis of small-tip-angle excitation," *J Magn. Reson.*, Vol. 81, 43–56, 1989.
5. Katscher, U., P. Börnert, C. Leussler, and J. van den Brink, "Transmit sense," *Magn. Reson. Med.*, Vol. 49, No. 1, 144–150, 2003.
6. Zhu, Y., "Parallel excitation with an array of transmit coils," *Magn. Reson. Med.*, Vol. 51, No. 4, 775–784, 2004.
7. Saekho, S., F. E. Boada, D. C. Noll, and V. A. Stenger, "Small tip angle three-dimensional tailored radiofrequency slab-select pulse for reduced B_1 inhomogeneity at 3T," *Magn. Reson. Med.*, Vol. 53, No. 2, 479–484, 2005.

8. Ullmann, P., S. Junge, M. Wick, F. Seifert, W. Ruhm, and J. Hennig, "Experimental analysis of parallel excitation using dedicated coil setups and simultaneous RF transmission on multiple channels," *Magn. Reson. Med.*, Vol. 54, No. 4, 994–1001, 2005.
9. Setsompop, K., L. L. Wald, V. Alagappan, B. Gagoski, F. Hebrank, U. Fontius, F. Schmitt, and E. Adalsteinsson, "Parallel RF transmission with eight channels at 3 tesla," *Magn. Reson. Med.*, Vol. 56, No. 5, 1163–1171, 2006.
10. Graesslin, I., P. Vernickel, J. Schmidt, C. Findeklee, P. Röschmann, C. Leussler, P. Haaker, H. Laudan, K. M. Luedeke, J. Scholz, S. Buller, J. Keupp, P. Börnert, H. Dingemans, G. Mens, G. Vissers, K. Blom, N. Swennen, L. Mollevanger, P. Harvey, and U. Katscher, "Whole body 3T MRI system with eight parallel RF transmission channels," *14 Proceedings of International Society of Magnetic Resonance in Medicine*, 129, Seattle, USA, May 2006.
11. Vernickel, P., P. Roschmann, C. Findeklee, K. M. Ludeke, C. Leussler, J. Overweg, U. Katscher, I. Graesslin, and K. Schuenemann, "Eight-channel transmit/receive body MRI coil at 3T," *Magn. Reson. Med.*, Vol. 58, No. 2, 381–389, 2007.
12. Yarnykh, V. L., "Actual flip-angle imaging in the pulsed steady state: A method for rapid three-dimensional mapping of the transmitted radiofrequency field," *Magn. Reson. Med.*, Vol. 57, No. 1, 192–200, 2007.